Potency of Severe Plastic Deformation Processes for Optimizing Combinations of Strength and Electrical Conductivity of Lightweight Al-Based Conductor Alloys

Maxim Yu Murashkin, Nariman A Enikeev, Xavier Sauvage

Materials Transactions, Vol. 64, No. 8 (2023) pp. 1833 to 1843
Special Issue on Superfunctional Nanomaterials by Severe Plastic Deformation

Review

Potency of Severe Plastic Deformation Processes for Optimizing Combinations of Strength and Electrical Conductivity of Lightweight Al-Based Conductor Alloys

Maxim Yu. Murashkin[1,2], Nariman A. Enikeev[1,2] and Xavier Sauvage[3,*]

[1]*Institute of Physics of Advanced Materials (M.M.)/Laboratory of Metals and Alloys under Extreme Impacts (N.E.), Ufa University of Science and Technology, Zaki Validi, 450076 Ufa, Russia*
[2]*Laboratory of Dynamics and Extreme Characteristics of Promising Nanostructured Materials, Saint Petersburg State University, Peterhof, St. Petersburg, 198504, Russia*
[3]*Univ Rouen Normandie, INSA Rouen Normandie, CNRS, Groupe de Physique des Matériaux UMR 6634, 76000 Rouen, France*

This paper presents an overview of fundamentals and potential applications of ultrafine-grained Al-based conductors developed with the help of severe plastic deformation (SPD) techniques. Based on deliberate formation of nanoscale features (such as nanoprecipitates, segregation of solutes along crystallographic defects and so on) within ultrafine grains, it is possible to optimise their mechanical and functional performance enhancing the combination of strength and electrical conductivity to produce advanced lightweight conductors required by modern industries. Guidelines related to SPD-driven development of Al alloys with properties superior to those exhibited by traditionally processed conductors are discussed. [doi:10.2320/matertrans.MT-MF2022048]

(Received March 10, 2023; Accepted April 13, 2023; Published May 19, 2023)

Keywords: *severe plastic deformation, ultrafine-grained structures, electrical conductivity, mechanical strength, electrical conductors, Al alloys*

1. Introduction

There is a continuous increase of the electric power consumption across the world and the unavoidable future reduction of fossil energy will further promote this growth thanks to the development of solar or wind energy for example. Electrical conductors are key components, they have to be easily shaped in proper dimensions, they have to be reliable, affordable and minimize power loss by Joule Effect. Conductors are usually made of metals or metallic alloys, ductile materials suitable for forming processes. Silver exhibits the highest electrical conductivity ($1.6 \times 10^{-8}\,\Omega\,m$) but is too expensive, therefore Copper, with a slightly lower electrical conductivity ($1.7 \times 10^{-8}\,\Omega\,m$), is widely used. There are however some concerns about future copper supply and price. Besides, in applications where low weight is required, there is a need for low weight conductors pushing the development of aluminium-based materials.[1)] Materials with a high specific strength combined with a low electrical resistivity are of interest both for transportation industries and for power transmission lines. For example, modern cars can contain up to 5 km of wiring comprising a significant weight, so that developing advanced Al-based conductors can assist reducing the weight and cost of automobiles together with lowering environmental impact and improving fuel efficiency.[2)] Pure aluminium exhibits an electrical conductivity of only 62% of that of copper but with a much lower density (three times less) and is available at a much lower price. Up to the end of the 20th century, the use of Al conductors has been limited to few specific applications because it is more difficult to process and because of the high resistivity of the Al_2O_3 oxide that inevitably grows on surface that leads to connecting problems. Power transmission lines are among the most important and the most advanced use of Al conductors. Specific designs of cables reinforced with steel wires have been developed to optimize the combination of electrical conductivity and mechanical strength (including fatigue properties). The demand for such components that combine low weight, high mechanical strength and high electrical conductivity has dramatically increased during the past years[1)] and will continue to do so with the rise of electric power vehicles and other advanced transportation applications.

Increasing the mechanical strength of Al requires the design of microstructures with obstacles to the motion of dislocations, such as solid solution, forest dislocations (strain hardening), grain boundaries, precipitates. However, all these features may scatter conduction electrons and thus affect the electrical conductivity. Solid solution hardening is never used for the design of alloys where a high electrical conductivity is required because the homogeneous distribution even of a small amount of alloying elements has the most detrimental effect on the electrical conductivity. Dislocations, however, have a moderate influence. It has been shown that a dislocation density up to of $10^{16}\,m^{-2}$ gives rise to an increase of only about 10% of the electrical resistivity.[3)] Commercially pure Al alloys (AA1350 for example) are typically used in as-drawn state, with a high dislocation density leading to a tensile stress up to 200 MPa. This is however not sufficient for power transmission lines that are typically made of 6xxx aluminium alloys where Mg and Si are the main alloying elements leading to a high density of second phase particles after appropriate precipitation treatment. They typically exhibit a tensile stress in the range of 245–330 MPa with an electrical conductivity of 57.4–52.5% IACS (International annealed Copper Standard).[4)]

Taking advantages of grain boundaries (GB) to design optimized microstructures for unique combination of strength and electrical conductivity, has been only possible thanks to the development of Severe Plastic Deformation Processes

*Corresponding author, E-mail: xavier.sauvage@univ-rouen.fr

(SPD).[5] It is now well admitted that such process may be applied at large scale to produce ultrafine grained materials with grain sizes ranging from 50 to 500 nm.

As proposed by Mayadas *et al.*,[6] the contribution of GBs to the electrical resistivity writes as:

$$\rho^{GB} = \frac{\rho^{0}_{Al}}{3\left(\frac{1}{3} - \frac{\alpha}{2} + \alpha^2 - \alpha^3 \, ln\left(1 + \frac{1}{\alpha}\right)\right)} \quad (1)$$

With

$$\alpha = \frac{\lambda R}{d(1-R)} \quad (2)$$

Where λ is the mean free path of electrons in Al ($\lambda = 18.9\,\text{nm}$[7]), and R the reflection coefficient of grain boundaries. In metals, R is often close to 0.5[8] and experimental data indicate that R is in a range of 30 to 50% in pure Al.[9,10] For a grain size of 25 nm, eq. (1) gives an estimate of the contribution of GBs to the electrical resistivity of about $2 \times 10^{-8}\,\Omega\,\text{m}$ which is significant comparing to the intrinsic electrical resistivity of pure Al ($2.65 \times 10^{-8}\,\Omega\,\text{m}$). However, it quickly drops at larger grain sizes down to about 0.50 and $0.25 \times 10^{-8}\,\Omega\,\text{m}$ for d = 100 and 200 nm respectively.

The contribution of GBs to the yield stress (σ_y) of metals has been studied many years ago and is known as the "Hall and Petch law":

$$\sigma_y = \sigma_0 + \frac{k}{\sqrt{d}} \quad (3)$$

Where σ_0 is the lattice friction stress, d is the grain size and k is a constant.

Thus, decreasing the grain size increases the yield stress and the extrapolation of the data of Hansen *et al.*[11] shows that a maximum yield stress of about 250 MPa could be achieved for a grain size of 25 nm in pure Al. Note, that the Hall-Petch slope for SPD materials defined by the grain boundary strengthening is still a widely disputable issue since this contribution might be interfered by the effects of the other structural factors. The most recently reported results by Dangwal *et al.*,[12] who analyzed numerous experimental data, testify that k may be considerably increased even for commercially pure aluminuim. These observations are consistent with the model for the deformation behavior of metals accounting for dislocation-mediated grain boundary sliding.[13] Wenwu Xu *et al.*[14] have shown that significant deviation to the Hall and Petch law may occur at such small grain size and the yield stress might be up to 1 GPa. This work is however based on molecular dynamic simulation carried out at very strain rate and cannot be compared with classical tensile experimental data.

Anyway, achieving such small grain sizes by SPD in high purity Al is not realistic due to the high driving force for grain growth and the relatively high mobility of grain boundary during deformation at room temperature.[15] Therefore, the design of UFG materials with an optimized combination of electrical and mechanical properties that takes advantage of GBs usually relies on multiple factors such as intergranular precipitates and GBs or intragranular precipitates and GBs or composite UFG structures. In this short overview, it is proposed to report about the most promising approaches that enable to reach various combinations of mechanical strength and electrical conductivity adapted to various application thanks to SPD applied to Al-based materials.

2. Application of SPD Processes to Traditional Al Alloying Systems for Enhanced Combination of Mechanical Strength and Electrical Conductivity

Traditional approaches to design high performance Al-based conductor alloys assume two main approaches: (i) Using solid solution treatment with subsequent controlled heat treatments for decomposing the solid solution and achieving precipitation of finely dispersed particles entailing precipitation hardening; (ii) Using the alloying systems with low solubility to avoid the solid solution formation with formation of fine intermetallic phase pinning grain boundaries to increase the thermal stability of the material for specific applications. Below we consider how SPD-based procedures can intensify the benefits of the traditional approaches on the example of the most popular Al–Mg–Si system (6xxx series) and Al–Zr alloys with low Zr content.

2.1 Age-hardenable Al–Mg–Si alloys

Age-hardenable 6xxx alloys are used as the most popular Al-based conductors with highest strength maximally approaching strength of Cu conductors (Ultimate tensile strength (UTS) of 400–430 MPa) after traditional thermal-mechanical treatments (TMT) such as T81.[4] Their conductivity is approaching the level of Commercially Pure (CP) Al and 6xxx series alloys are the most demanded Al-based conductor material in the industry. Wires fabricated of 6xxx alloys are being widely used in different electrotechnical applications including automotive industry or self-bearing stand-alone wires. Traditional TMT (EN 50183:2002)[16] include solid solution treatment after casting followed by natural ageing, wire drawing and final ageing to control the combination of properties by decomposition of solid solution and precipitation of strengthening particles. To extend the domain of properties combination, several studies proposed variations of the standard T81 treatment[17–19] by involving specific artificial ageing before the final cold drawing. Table 1 summarizes data from the literature for conventionally and SPD-treated 6xxx alloys.

Introducing SPD processing gives an additional possibility to control mechanical and functional properties by adjusting the grain size and grain boundaries features (misorientation, size, local chemical composition).[5] SPD processes may also modify diffusional processes intensifying atomic transport and promoting deeper decomposition of solid solution as well as facilitating unconventional dynamic and static precipitation. These features might help producing materials with a simultaneous increase of both mechanical strength and electrical conductivity which can be superior to the properties exhibited by traditionally treated conductor alloys (Table 1). Among the SPD techniques listed in Table 1, HPT stands for high-pressure torsion, ECAP – for the equal-channel angular pressing and ECAP-C – continuous ECAP process according to the Conform scheme.[5]

Table 1 Mechanical properties and electrical conductivity of conventionally treated and SPD-processed Al–Mg–Si alloys.

Alloy (wt.%)	Process/ Treatment	σ_{UTS}, MPa	$\sigma_{0.2}$, MPa	δ, %	% IACS	Ref.
After conventional or modified treatment						
AA6101 or AA6201	Combined casting, rolling, solution treated, drawing and aging (T81)	245–342	-	3.0-3.5	57.4-52.5	4)
6101	Combined casting, rolling, solution treated, aging and drawing	375	-	-	56.0	17)
Al-1.0Mg-0.5Si-0.8Cu	Combined solution treated, aging, rolling and aging	316	-	-	57.4	18)
6201	Combined casting, hot extruded, solution treated and cold rotary swaging	424.4	410.7	6.71	52.78	19)
After the SPD-assisted treatment						
6201	Combined solution treated and two-stage HPT	412	-	4.9	55.6	21)
		365	-	8.8	58.4	
Al–0.60Mg–0.45Si	Combined solution treated, ECAP-PC and aging	289	275	14.0	56.1	28)
6063		308	289	15.5	58.6	20)
6063	Combined solution treated and two-stage ECAP	331	328	12.0	51.4	29)
6101	Combined solution treated, ECAP-C and T81-alike TMT	320-370	-	3.0	57.2-56.1	30)
	Combined solution treated and ECAP-C	308	282	15.1	53.1	31,32)
	Combined solution treated, ECAP-C and aging	304	291	15.0	57.1	
	Combined solution treated, ECAP-C, aging and drawing	364	-	3.5	56.4	
	Combined solution treated, ECAP-C and aging	238	-	16.0	57.0	33)
	Combined solution treated, aging, ECAP-C and drawing	385	-	-	55.1	17)

The initially proposed SPD-inspired strategy for achieving this goal was based on benefits of grain refinement accompanied with accelerated formation of nanoprecipitates. First, it was experimentally shown in Ref. 20) and further formulated in Refs. 21, 22) as represented in Fig. 1.

Sauvage *et al.*[22] proposed a quantitative basis to analyse the horizons for possible space of "strength-conductivity" combinations in UFG alloys and to predict the limits of the properties that can be achievable in Al–Mg–Si alloys by SPD (Fig. 2). As a result, SPD-driven formation of UFG structures with intragranular nanoprecipitates of different modifications was demonstrated as a highly fruitful approach to simultaneously improve the strength and electrical conductivity in this system.[22]

Important to note that several studies reported about grain boundary segregation in SPD-processed Al–Mg–Si alloys.[23–25] These atomic-scale features are essential for the SPD-processed alloys and may considerably contribute to additional impact in strength[26,27] as well as to depletion of solid solution.[25]

Most of the research above was carried out with small specimens mostly processed by HPT. These laboratory studies allowed to work out the necessary structural design which could be potentially up-scalable. Among the proposed approaches, the advanced ECAP technologies capable of introducing more strain per pass than traditional ECAP in parallel channels seems promising.[20,28] Another direction in the field is related to optimization of the SPD processing temperature leading to utilizing advantages of both dynamic and static ageing.[29] These studies logically led to a step up in producing UFG Al 6xxx semi-products in the form of wires by combining enhanced SPD (the continuous ECAP-C scheme, for example) with traditional routes such as drawing.[30–32] In addition to the improved static strength/conductivity ratio these wires demonstrated better fatigue properties[2,32,33] as compared to traditional TMT, which is important for automotive applications where vibrational loads are essential[2] or for the fretting fatigue issue.

However, there are still issues related to the possible negative effects of SPD nanostructuring on the functional properties of the 6xxx alloys. Rochet *et al.*[2,34] warned that the pitting corrosion behaviour of the ECAP-processed Al–Mg–Si alloys might be affected due to increased intergranular corrosion. This issue has to be kept in mind because wires can be subjected to the combined influence of aggressive environment which can be amplified by varying temperature and vibrational effects.[33]

2.2 Thermal resistant Al–Zr-based systems

For applications with operational temperatures of conductors above 90°C (a standard requirement for conventional Al wires[4]), eventually resulting from Joule effect in case of high power, Al-based conductors usually do not exhibit sufficient thermal stability. To overcome this issue, Al–Zr alloys with a Zr content up to 0.4 wt.%[35] have been developed for overhead conductors. However, the UTS of these conducting materials typically does not exceed 200 MPa (see Table 2 where the reference data on Al–Zr alloys subjected to conventional and SPD-assisted treatments are collected). Proposed doping the Al–Zr system with scandium[44,45] is not also capable to increase this value. This level of mechanical strength does not meet the raising demand from the industry. Unfortunately, the additional grain boundary strengthening resulting from SPD (HPT and ECAP) is relatively weak.[36–38] It is the result of the limited solubility of Zr in Al that do not promote grain refinement leading to mean grain sizes similar to CP Al processed by SPD (400–900 nm).

As shown in Ref. 39), the properties of Al–Zr alloys might be however improved by Mg doping, a lightweight element that does not affect conductivity as much as other solutes. Also, additives of this element, especially in low concentrations, do not impair the corrosion resistance of aluminum, which is important for conductive materials used without insulation. During SPD Mg dramatically increases the dislocation multiplication rate leading to much stronger grain refinement as compared to classical binary Al–Zr alloys.[40,41]

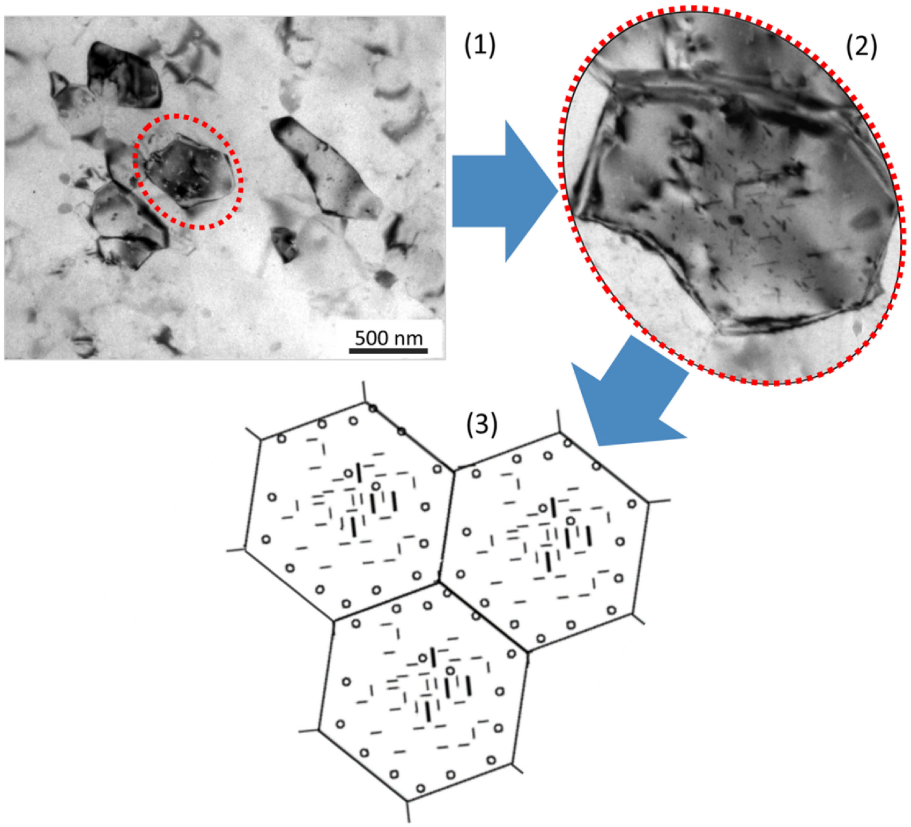

Fig. 1 Hierarchical structure comprising ultrafine grains (1) as well as stable and metastable precipitates in their interiors (2), which is produced by SPD and artificial ageing, and its schematic representation (3). Drawn according to a concept presented in Ref. 20).

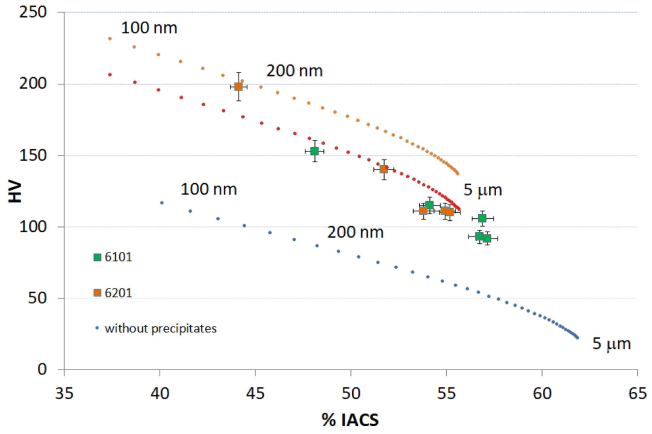

Fig. 2 General prediction of the combination of hardness and electrical conductivity (%IACS) for AlMgSi alloys as a function of the grain size and with 0.2 wt.% of solute left in solid solution. Reproduced from Ref. 22).

The strongest UFG state accompanied with reasonable conductivity (51.1%IACS) and thermal resistance (up to 150°C) was achieved in the Al–0.53Mg–0.27Zr alloy processed by HPT (Table 2). Such an unusually high level of strength for an alloy containing less than 1% magnesium, in addition to reduced grain size and increased dislocation density, may be due to the presence of nanoclusters and Mg segregations at grain boundaries, as reported in other alloys with similar magnesium content and processed by HPT.[42)]

Thanks to proper adjustment of the chemical composition, of the SPD process (by ECAP-C technique) and of aging treatments, it has been possible to achieve UFG structures with a relatively high strength ($\sigma_{UTS} = 267$ MPa), an electrical conductivity of 57.1% IACS and an operating temperature up to 150°C (much higher than the conventionally required limit of 90°C), see Table 2.

Recently, Nokhrin *et al.*[47)] suggested doping the Al–Zr system with other elements (Er, Si, Hf and Nb) and in combination with SPD they achieved the best "hardness-conductivity" trade-off (57.1%IACS, Hv = 482 MPa) with an Al–0.25%Zr–0.25%Er–0.20%Hf–0.15%Si alloy processed by ECAP and annealing. Further studies are required to check if this strategy might be cost-effective for the development of competitive alloys dedicated to electrical conductors.

3. Beyond Modified Commercial Alloys: The Potentiality of New Systems Processed by SPD

As shown above, SPD can provide additional possibilities to tune the combination of properties by adapting the chemical compositions of existing alloys, especially to promote grain refinement. Another strategy is to go beyond these classical alloys and explore new systems with high potential for the design of UFG electrotechnical alloys.

3.1 Al-RE alloys processed by SPD

Immiscible systems such as Al–RE (where RE stands for Rare Earth) alloys are potentially interesting. RE elements form second phase particles that can significantly strengthen the material and the extremely low solubility of RE does not

Table 2 Mechanical properties and electrical conductivity of conventionally treated and SPD-processed Al-based conductor materials alloyed with zirconium.

Alloy (wt.%)	Process/ Treatment	σ_{UTS}, MPa	$\sigma_{0.2}$, MPa	δ, %	% IACS	Texpl. °C	Ref.
After conventional or modified treatment							
Al-0.1...0.3Zr	Conventional thermomechanical process	169-250	-	1.5-2.0	55-60	150-230	35)
Al-0.15Zr	Combined casting, rolling and extrusion process and drawing	194-212	-	3.0	58.6-60.7	-	43)
Al-0.6Zr	Combined electromagnetically casting (EMC) and cold drawing	234	207	6.8	55.6	230	39)
Al-0.23Zr-0.06Sc	Combined cold drawing and two-stage aging	194.3	167.6	-	61.4	-	44)
Al-Zr≤0.1Sc	Combined casting, rolling and drawing	188–197	-	-	58.0–59.5	310	45)
After the SPD-assisted treatment							
Al-0.4Zr	Combined casting, rolling and HPT	190	140	23.2	47.4	-	36, 37)
	Combined casting, rolling, HPT and annealing at 230°C	275	265	7.7	52.0	-	37)
	Combined casting, rolling, aging and HPT	118	96	18.4	54.5	-	38)
	Combined casting, rolling, aging and HPT	163	149	19.0	54.9	-	
	Combined casting, rolling, aging and ECAP-C	193	178	19.5	59.6	-	46)
	Combined casting, rolling, aging, ECAP-C and drawing	226	199	5.5	59.6	150	
Al-0.53Mg-0.27Zr	Combined casting, rolling, aging and HPT	465	400	3.0	51.5	-	40)
Al-0.40Mg-0.20Zr	Combined casting, rolling, aging and ECAP-C	205	188	14.6	57.6	-	41)
	Combined casting, rolling, aging, ECAP-C and drawing	267	249	2.4	57.1	150	
Al-1.17Mg-0.34Zr	Combined casting, rolling, aging and ECAP-C	267	257	10.4	48.3	-	46)
	Combined casting, rolling, aging, ECAP-C and drawing	366	321	2.1	48.1	150	

affect the aluminum matrix electrical conductivity. The first processing route that has been proposed for this system was RE alloying up to several wt.% by powder metallurgy techniques,[48] a quite laborious and costly process. An alternative technique has been proposed more recently, it is based on electromagnetic casting (EMC) and ultrafast cooling.[49] The alloy synthesis is simplified but properties are not particularly interesting (Table 3).

Table 3 Mechanical properties and electrical conductivity of conventionally treated and SPD-processed Al–RE systems.

Alloy	Process/ Treatment	σ_{UTS}, MPa	$\sigma_{0.2}$, MPa	δ, %	% IACS	Texpl, °C	Ref.
After conventional treatment							
Al-RE	Combined casting, rolling and extrusion process (CREP)	200-250	-	≥9,0	58.6-55.6	-	43)
Al-7RE (01417 alloy)	RS/PM method	180-230	-	4.6-2.5	56-54	-	48)
	Combined casting, rolling, annealing, and drawing	226-233	-	0.8-1.0	52-56	-	49)
Al-0.20Sc-0.04Zr	Combined pre-aging, cold rolling, and aging	213.3	-	13.8	61.7	345	55)
After the SPD-assisted treatment							
Al-2.5RE	Combined EMC and HPT	297	265	18.5	56.6	-	52)
	Combined EMC, HPT and annealing (230°C)	225	195	21.6	60.2		
Al-4.5RE	Combined EMC and HPT	580	489	17.3	45.5	-	51, 52)
	Combined EMC, HPT and annealing (230°C)	582	520	12.0	50.3	210	
	Combined EMC, HPT and annealing (280°C)	522	455	17.0	52.2	210	
	Combined EMC, annealing and HPT	435	410	30.0	50.2	150	52)
	Combined EMC, annealing, HPT and annealing (230°C)	430	320	17.0	55.9	150	
Al-8.5RE	Combined EMC and HPT	637	506	18.2	39.7	-	50, 51)
	Combined EMC, HPT and annealing (230°C)	670	506	12.4	43.1	210	
	Combined EMC, HPT and annealing (280°C)	620	460	13.7	44.7	210	
Al-0.5Sc-0.5Mg	Combined ECAP and annealing	245	-	-	~52	-	58)

Using SPD, Murashkin *et al.*[50] showed for the first time that HPT can produce an UFG structure in Al–8.5% (Ce/La) alloy with a significant amount of RE atoms in super saturated solid solution in the Al matrix. Then, this specific UFG state can potentially be treated as an age-hardenable

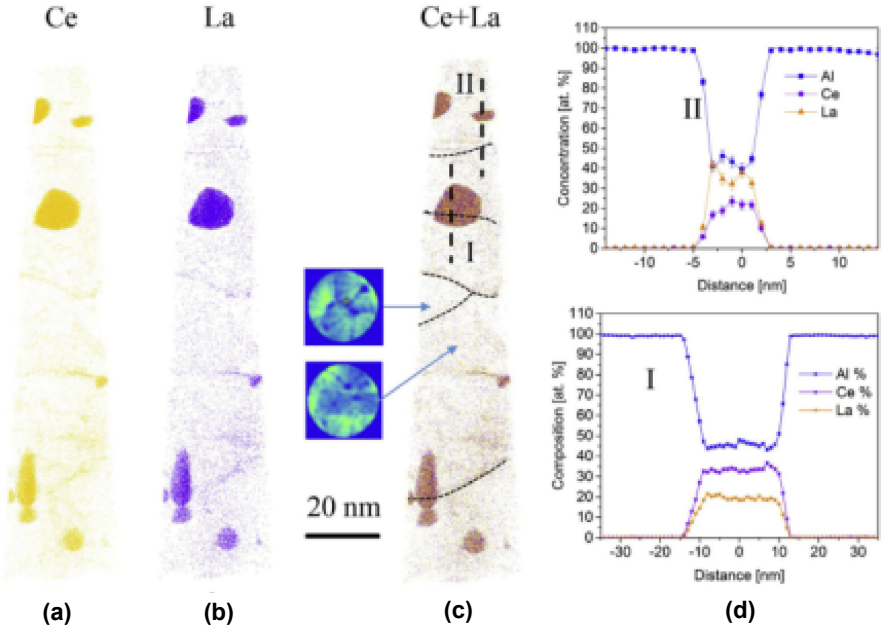

Fig. 3 Nano-scaled structure of an Al–RE alloy processed by SPD. Atom probe tomography data showing nanoparticles and GB segregations of RE elements: Ce (a) and L (b) as well as of their combination (c). Concentration profiles of Ce/La recorded along lines I and II (d). Reproduced with permission from Ref. 52).

alloy. Following this route, subsequent studies[51–53] SPD and heat treatment parameters were optimized to combine UFG structure and nanoscaled precipitates (Fig. 3) giving rise to promising combinations of strength and conductivity (Table 3).

As was shown in Refs. 54–56), Al–Sc is another potential interesting system for the design of heat-resistant conductors. Zhou *et al.*[55] showed that combination of traditional treatments (such as aging and cold drawing) for the Al–0.2Sc–0.04Zr alloy may lead to a UTS of 213 MPa combined with an electrical conductivity of 61.7% IACS with a thermal stability up to 345°C (Table 3). These excellent properties result from the precipitation of nanoscaled $Al_3(ScZr)$ precipitates that efficiently pin GBs.[57]

However, despite their high electrical conductivity and heat resistance, Al–Sc alloys do not exhibit outstanding strength, to more classical Al–Zr alloys (Table 3). Following the strategy proposed for Al–Zr (see the section above) Chuvil'deev *et al.*[58] proposed to introduce a small amount of Mg in combination with SPD processing via ECAP. It led to a significant strengthening with a tensile strength up to 245 MPa with an acceptable level of electrical conductivity of 52–54% IACS and a good thermal stability.

3.2 Al–Fe alloys processed by SPD

Processing by SPD immiscible systems like Al–Zr or Al–RE has been proven to be a promising approach to achieve ultrafine grained structure with low solute content in the matrix and a reasonable thermal stability thanks to second phase nanoparticles. Thus, appropriate processing and thermal treatments can give rise to excellent combination of strength and electrical conductivity. However, such systems have a main drawback, which is the price. Besides, the limited solubility of Zr in Al for example, also limits the range of reachable properties. Therefore, to go further, it has been proposed to take advantage of SPD not only to reduce the grain size but also to create super saturated solid solutions by mechanical mixing. The Al–Fe system is probably the most interesting system to develop this approach for several reasons: i) the solubility limit of Fe near room temperature is extremely low,[59] thus this alloying element is not supposed to affect significantly the electrical resistivity, ii) Fe is an abundant and cheap element, iii) aluminum scraps often contain significant Fe amount, thus taking advantage of Fe may simplify recycling. The Al–Fe system is the typical base for 8### aluminum alloys, but the typical Fe amount does not exceed 1 wt.%. Besides, intermetallic particles that nucleate and grow during classical solidification processes are relatively coarse (micrometer scale) and cannot efficiently stabilize an UFG structure. However, it has been shown that these brittle intermetallic Al_6Fe or $Al_{13}Fe_4$ particles[60] are progressively fragmented under large level of deformations.[61–66] Then, the typical grain sizes achieved by SPD are typically in a range of 100 to 400 nm.[61,64,66] For the highest level of deformation, Senkov *et al.* were the first to report the formation of super saturated solid solutions induced by strain induced decomposition of the intermetallic phase.[67] Similar features have been reported in an Al–5Fe alloy processed by ECAP where the authors report about a super saturated solid solution of 0.6 wt.% Fe in Al and a significant age hardening response.[64] More recently, Atom Probe Tomography (APT) data combined with transmission electron microscopy (TEM) observations confirmed the mechanisms leading to the progressive strain induced dissolution of intermetallic phases.[68] In the same work, *in-situ* TEM data also revealed how post-deformation thermal treatments promote the nucleation of new intermetallic particles that pin GBs.

In an Al–2Fe alloy processed by HPT, Medvedev *et al.* managed to obtain an UFG structure with a yield stress of

320 MPa combined with an electrical conductivity as high as 52% IACS.[69] These properties were obtained by SPD at 200°C which seems the most effective way to directly obtain ultrafine grains and uniform distribution of nanoscaled intermetallic particles without significant amount of Fe left in super saturated solid solution.[69]

It has also been demonstrated that the initial microstructure resulting from casting of the Al–Fe alloy (size, volume fraction and crystallographic structure of intermetallic particles) has a strong influence on the final structures and properties achieved thanks to SPD.[61,65,69] It should be noted that a fine eutectic structure gives rise to the best combination of strength, ductility and electrical conductivity after HPT. And the same authors have shown that appropriate post-SPD aging can promote further hardening such as in age hardenable aluminum alloys[66] (see Table 4).

Thus, the synergy of novel casting technologies (such as EMC) which allow the easy production of different eutectic morphology (Fig. 4), combined with advanced SPD processing techniques[70] seems particularly promising (Table 4). For example, one may note that Al–Fe alloys produced by EMC and processed by ECAP/cold rolling exhibit a similar thermal stability like Al–Zr alloys,[73] with a tensile strength close to that of 6xxx alloys!

3.3 Al–Ca alloys processed by SPD

The Al–Ca system is also offering some interesting possibilities for the design of low weight electrical conductors with a similar strategy because: i) the solubility of Ca in Al is also extremely low; ii) Ca is an abundant element, iii) Ca is a low weight element. Like for the Al–Fe alloys, casted Al–Ca alloys with intermetallic particles (Al_4Ca) can be processed by SPD to promote the fragmentation of particles. Following this route, Rogachev *et al.* have shown that the processing of an Al–8Ca alloy by HPT may give rise to a mean grain size of only 30 nm with a hardness up to 1.9 GPa.[74] To achieve a homogeneous distribution of Ca within the UFG structure, Sauvage *et al.* have proposed another approach, starting from an Al–Ca composite and using SPD to create mechanical mixing without phase transformation (dissolution of Al_4Ca).[75] The result is a nanoscaled structure with a grain size of only 20 nm stabilized by intensive Ca segregation at GBs (Fig. 5). Such segregations promote hardening with a strong deviation to the Hall and Petch law and an estimated yield stress up to 1 GPa. However, these segregations strongly scatter electrons, giving rise to a high electrical resistivity ($2 \times 10^{-7}\,\Omega\,m$), thus low temperature annealing is required to reach an acceptable properties combination through the nucleation of nanoscaled Al_4Ca particles along GBs.

Table 4 Mechanical properties and electrical conductivity of conventionally treated and SPD-processed Al–Fe system.

Alloy	Process/ Treatment	σ_{UTS}, MPa	$\sigma_{0.2}$, MPa	δ, %	% IACS	Ref.
After conventional treatment						
AA8030, 8176	Combined casting, rolling and drawing	103-152	-	10	60.6-61	71)
After the SPD-assisted treatment						
Al-2Fe	Combined casting and HPT	649	564	5.0	40.3	61,69)
	Combined casting, HPT and annealing	335	310	13.5	49.3	69)
	Combined casting and two-stage HPT	327	295	14.2	52.3	
Al-4Fe	Combined casting and HPT	340	270	8.0	48.0	61)
Al-5Fe	Combined ECAP with backpressure	244	216	5.8	-	64)
	Combined ECAP with backpressure and aging	272	257	1.5	-	
AA8176	Combined casting, heat treatment and ECAP (RT)	172.2	157.9	11.8	60.88	72)
	Combined casting, heat treatment and ECAP (150°C)	185.7	164.9	7.6	59.97	
	Combined casting, heat treatment and two-stage ECAP	-	178	11.2	61.55	
Al-0.5Fe	Combined EMC and ECAP	156	121	19.8	57.2	73)
	Combined EMC, ECAP and rolling	200	185	17.2	58.5	
	Combined EMC, ECAP, rolling and annealing	195	175	16.5	59.6	
Al-2.5Fe	Combined EMC and ECAP	258	200	15.8	45.5	
	Combined EMC, ECAP and rolling	340	290	16.7	47.9	
	Combined EMC, ECAP, rolling and annealing	330	275	16.5	49.3	

4. Metal Matrix Composites Processed by Severe Plastic Deformation

As reviewed above, SPD-related approaches for the processing of high strength lightweight conductors rely on the optimization of alloys microstructure (grain size, precipitation morphology and distribution, solid solution decomposition, defect configurations). Alternatively, composite materials taking benefits of two or more metallic constituents can be processed by SPD to develop Al-based conductors with enhanced static and fatigue strength, electrical conductivity and thermal stability.

Al-based composites can be composed of different components. Tian *et al.*[76] proposed a metal-matrix composite based on the Al–Ca system, produced by a technique combining powder metallurgy and complex SPD processing. As a result, Ca particles were transformed to nanofilaments with a volume fraction of 20% allowing the combination of a low density, a high strength and a reasonable conductivity

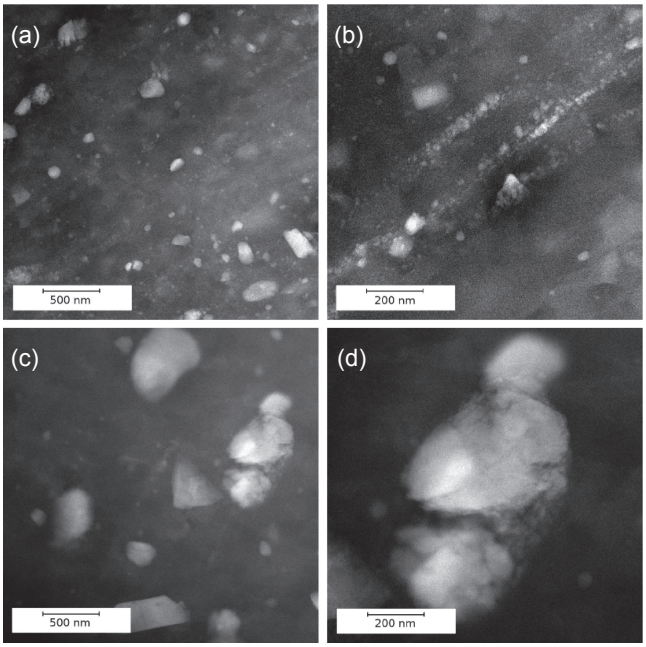

Fig. 4 Al–2Fe (a, b) and Al–4Fe (c, d) alloys processed by HPT. STEM HAADF images showing the fragmentation of intermetallic particles (brightly imaged). Reproduced from Ref. 61).

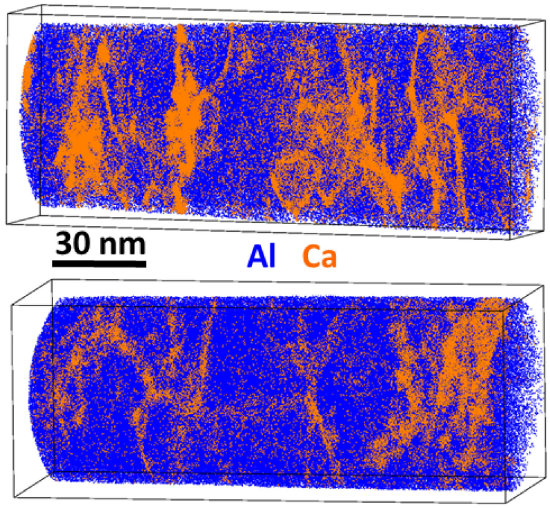

Fig. 5 Nanoscaled structure of an Al–Ca composite processed by HPT. Atom Probe Tomography data showing segregation of Ca along GBs (Ca orange, Al blue). Reproduced from Ref. 76).

of the final composite.[76] The UTS of such composite can reach an outstanding level of 470 MPa, however, the ductility was significantly sacrificed and the multistep processing technology is rather laborious.

Authors of Ref. 77) proposed to reinforce pure Al by oxide, boride or carbide nano- and micro-particles (Al_2O_3, TiB_2, TiC) by using mechanical mixing followed by ECAP. They reported a positive influence of TiB_2 particles that enhance mechanical properties without a notable reduction of conductivity (about 54% IACS). ECAP promote an homogeneous distribution of particles in the matrix and in turn they apparently do not affect significantly the mean free path of electrons. Unfortunately, the YS and UTS remain relatively low (as compared to other systems described in previous sections) with maximal values of only 103 and 165 MPa, respectively.

Recently, SPD-processed bimetallic systems attracted more interest. In Ref. 78) it was shown that ECAP might be effectively used to adjust the combination of strength and electrical conductivity of a 6201 composite conductor with a 316 stainless steel core (UTS in a range of 390–590 MPa and 43–24% IACS). Unfortunately, if the strength is relatively high, the conductivity of such bimetallic composite is poor and the steel core significantly affect the weight.

Al–Cu composite wires made of an Al core coated with copper (known as copper clad aluminum wires) are well documented in the literature,[79] and they exhibit a typical electrical conductivity of 62% IACS combined with UTS of 252 MPa. The most recent publications on SPD-driven design of UFG Al/Cu bimetallic composites also showed promising results thanks to ECAP[80] or to high pressure torsion extrusion/reciprocal extrusion/twist extrusion.[81] Two ECAP passes provided a significant strengthening with a conductivity up to 60% IACS and even 68% IACS after annealing which was higher than theoretically predicted.

More complex helicoidal structures were created by various SPD-assisted extrusion processes.[81] Depending on the process and on the heat treatment, the authors managed to reach a remarkable level of conductivity combined with an increased load-bearing capacity for cylinders of pure Al reinforced with a spiral CP Cu armature. However, the large proportion of interphase boundaries promotes the nucleation of intermetallic phases (θ-Al_2Cu, γ-Al_4Cu_9 and ξ-Al_3Cu_4) and because of their low electrical conductivity, the final electrical conductivity of the wires might be significantly reduced.[82]

The elaboration of Al–Al based composite wires seems another interesting strategy. In Ref. 83) the authors have proposed to use a core made of AA1350 with high electrical conductivity and a clad made of AA6201 alloy with enhanced strength. The experimental strength values of this composite wire correlate well with estimates calculated thanks to the additive rule of mixtures. However, the combination of strength and electrical conductivity is not beyond that of classical AA6201.

As pointed out in subsection 2.2, the problem of increasing the thermal resistance of Al-based conductors is usually solved by alloying Al with small amount of Zr (typically 0.4 wt.%), while SPD promote strengthening by Mg doping. In Ref. 46) the possibility of creating a strong and thermally resistant composite wire with a UFG structure based on Al–Zr and Al–Mg–Zr alloys was considered. The wire core was made of Al–Zr alloy with high electrical conductivity, and the wire clad was of Al–Mg–Zr alloy with a potential high strength. To maximize the clad, the Mg content was increased more than 2.5 times as compared to the alloy in Ref. 40). This study demonstrates that this approach is very promising to produce high-strength heat-resistant conductors. Indeed, specific SPD processing led to a UTS of 354 MPa, an electrical conductivity of 50.6% IACS, and an operating temperature of up to 150 C. These excellent properties are the result of the UFG structure and of the homogeneous distribution of nanosized Al_3Zr particles. They are noticeably superior to those of classical Al–Mg–Si alloys widely used in

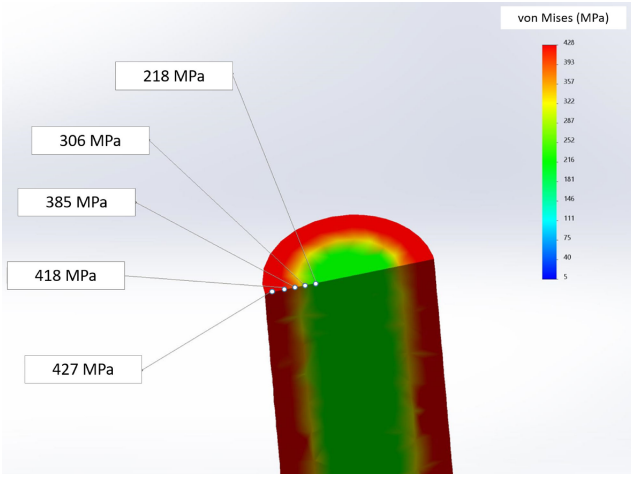

Fig. 6 Stress diagram of a two-component conductor, a longitudinal cross-section, re-drawn from the data presented in Ref. 85).

electrical engineering. A similar approach might be applied with other alloying elements such as Cu and Mn.[84)]

Traditionally, the properties of composite conductors are evaluated by the rule of mixtures in accordance with the volume fraction of each constituent. Authors of Ref. 85) used FEM simulation to evaluate the rational design of a two-component conductor in the form of a wire (Fig. 6) made of nanostructured high-strength alloy 6101 and aluminum electrical grade 1350. It was shown that the optimal combination of strength and electrical conductivity is achieved for a ratio between the core and the wire section of 0.16.

5. Concluding Remarks

The design of high strength and high conductivity metallic conductors has always been a challenge for scientists since defects are required to promote strengthening but they also scatter conducting electrons. The increasing demand for low cost, low weight, high strength and high conductivity wires and conductors is a strong motivation to investigate all the potentiality offered by Al based materials. A vital qualitative step-up from laboratory-scale applications to industrial solutions implies upscaling of existing processing approaches. The development of SPD techniques during the past 25 years, including the design of continuous processes like ECAP-Conform has open a new field for the development of UFG Al based electrical conductors. Recent developments in upscaling and modernizations of SPD techniques also provide new possibilities of optimizing technological routes[86,87)] and producing bulk workpieces[88)] attractive for industrial reproduction.

Note that despite intensive research in the area there are still poorly explored fields in development of SPD-designed conductor alloys. For example, creep properties. The creep issue can be really important for cable applications in long power lines due to the cable own weight and long distance between supports which causes high tensile stresses for long-term periods of operation. As recently summarized in Ref. 89), UFG materials can exhibit deterioration of creep properties depending on creep conditions and testing modes, which is demonstrated also on the example of ECAP-processed commercially pure Al and Al–Sc alloys[90,91)] and related to facilitation of grain boundary processes. This issue needs in a thorough dedicated research on the SPD-designed conductor alloys and it can be expected to be solved via deliberate precipitate engineering to tune misfit parameters combining APT analyses and DFT computations.[92)]

In this review, it has been shown how it is possible to explore combinations of chemical compositions, microstructures, processing routes and thermal treatments. Maximizing GB strengthening requires solute or nanoscaled particles to promote structure refinement and/or to stabilize the UFG structure and achieve good thermal stability. Severe plastic deformation can help creating super saturated solid solutions that cannot be achieved by classical thermal treatments and that can be decomposed during annealing for additional precipitate hardening or GB pinning. Severe plastic deformation promotes the segregation of some solutes along crystalline defects, decreasing the solubility and thus eventually enhancing the electrical conductivity of the Al matrix. Severe plastic deformation is very efficient for the fragmentation of second phase particles (intermetallic particles for example), leading to homogeneous distribution of nanoscaled fragments that promote mechanical strength and pin GBs. Severe plastic deformation creates numerous crystalline defects that modify precipitation kinetics and offer new possibilities for precipitation hardening alloys. These different strategies could be applied to classical commercial alloys to reach new combination of strength and electrical conductivity (like in 6xxx alloys). However, the most promising routes are those that involve the design of new alloys. Standard compositions might be adapted to promote some of the mechanisms described above, like doping with Mg of Al–Zr alloys to promote grain refinement. New alloys may also be specifically designed for SPD processes, like the Al–RE alloys that take advantage of the strong fragmentation of RE rich particles during SPD as well as cheaper Al–Fe based systems pre-produced with novel casting technologies. Finally, composite materials, even if they are more complex to elaborate, they also offer some interesting possibilities. For example, when wires have to sustain bending or torsion stresses, the design of graded structures or specific architectures thanks to adapted SPD processed might be a promising route for the design of optimized Al based low weight conductors.

To sum up, SPD-driven microstructural design proved to be a powerful pathway to develop lightweight high-performance Al-based electrical conductors with the properties superior to the level achieved by traditional approaches.

Acknowledgements

N. Enikeev and M. Murashkin acknowledge support from the Russian Ministry of Science and Higher Education (state assignment FEUE-2023-0007).

REFERENCES

1) Y. Wang, L. Zhu, G. Niu and J. Mao: Adv. Eng. Mater. **23** (2021) 2001249.

2) C. Rochet, E. Andrieu, B. Arfaei, J.-P. Harouard, A. Laurino, T.C. Lowe, G. Odemer and C. Blanc: Int. J. Fatigue **140** (2020) 105812.
3) J. Schrank, M. Zehetbauer, W. Pfeiler and L. Trieb: Scr. Metall. **14** (1980) 1125–1128.
4) F. Kiessling, P. Nefzger, J.F. Nolasco and U. Kaintzyk: *Overhead Power Lines: Planning, Design, Construction*, (Springer, Berlin, 2003) p. 759.
5) K. Edalati *et al.*: Mater. Res. Lett. **10** (2022) 163–256.
6) A.F. Mayadas, M. Shatzkes and J.F. Janak: Appl. Phys. Lett. **14** (1969) 345.
7) D. Gall: J. Appl. Phys. **119** (2016) 085101.
8) H. Schwarz and R. Lück: Mater. Sci. Eng. **5** (1970) 149–152.
9) P.V. Andrews, M.B. West and C.R. Robeson: Philos. Mag. **19** (1969) 887–898.
10) M.B. Kasen: Philos. Mag. **21** (1970) 599–610.
11) N. Hansen: Scr. Mater. **51** (2004) 801–806.
12) S. Dangwal, K. Edalati, R.Z. Valiev and T.G. Langdon: Crystals **13** (2023) 413.
13) R.B. Figueiredo and T.G. Langdon: J. Mater. Res. Technol. **14** (2021) 137–159.
14) W. Xu and L.P. Dávila: Mater. Sci. Eng. A **710** (2018) 413–418.
15) Y. Ito, K. Edalati and Z. Horita: Mater. Sci. Eng. A **679** (2017) 428–434.
16) EN 50183: *Overhead power line conductors – Bare conductors of aluminium alloy with magnesium and silicon content*, (European Standard, 2002).
17) M.Yu. Murashkin and I.V. Smirnov: Patent RU 2749601 *Methods for thermomechanical treatment of conductive Al–Mg–Si system alloys*, (Effective date for property rights: 13.12.2019).
18) C.H. Liu, J. Chen, Y.X. Lai, D.H. Zhu, Y. Gu and J.H. Chen: Mater. Des. **87** (2015) 1–5.
19) H. Jin, R. Guan, X. Huang, Y. Fu, J. Zhang, X. Chen, Y. Wang, F. Gao and D. Tie: J. Mater. Sci. Technol. **96** (2022) 226–232.
20) E.V. Bobruk, M.Yu. Murashkin, V.U. Kazykhanov and R.Z. Valiev: Rev. Adv. Mater. Sci. **31** (2012) 109–115.
21) R.Z. Valiev, M.Yu. Murashkin and I. Sabirov: Scr. Mater. **76** (2014) 13–16.
22) X. Sauvage, E.V. Bobruk, M.Yu. Murashkin, Y. Nasedkina, N.A. Enikeev and R.Z. Valiev: Acta Mater. **98** (2015) 355–366.
23) G. Nurislamova, X. Sauvage, M. Murashkin, R. Islamgaliev and R. Valiev: Philos. Mag. Lett. **88** (2008) 459–466.
24) X. Sauvage, M.Yu. Murashkin and R.Z. Valiev: Kovove Mater. **49** (2011) 11–15.
25) X. Sauvage, A. Duchaussoy and G. Zaher: Mater. Trans. **60** (2019) 1151–1158.
26) R.Z. Valiev, N.A. Enikeev, M.Yu. Murashkin, V.U. Kazykhanov and X. Sauvage: Scr. Mater. **63** (2010) 949–952.
27) S.V. Bobylev, N.A. Enikeev, A.G. Sheinerman and R.Z. Valiev: Int. J. Plast. **123** (2019) 133–144.
28) M. Murashkin, I. Sabirov, V. Kazykhanov, E. Bobruk, A. Dubravina and R.Z. Valiev: J. Mater. Sci. **48** (2013) 4501–4509.
29) N. Zhao, C. Ban, H. Wang and J. Cui: Materials **13** (2020) 1511.
30) V.Kh. Mann, A.Yu. Krokhin, I.A. Matveeva, G.I. Raab, M.Yu. Murashkin and R.Z. Valiev: Light Metal Age **72** (2014) 26–29.
31) M. Murashkin, A. Medvedev, V. Kazykhanov, A. Krokhin, G. Raab, N. Enikeev and R.Z. Valiev: Metals **5** (2015) 2148–2164.
32) A. Medvedev, A. Arutyunyan, I. Lomakin, A. Bondarenko, V. Kazykhanov, N. Enikeev, G. Raab and M. Murashkin: Metals **8** (2018) 1034.
33) R.C. Meagher, M.L. Hayne, J. DuClos, C.F. Davis, T.C. Lowe, T. Ungár and B. Arfaei: Increasing the Strength and Electrical Conductivity of AA6101 Aluminum by Nanostructuring. *Light Metals*, ed. by C. Chesonis, (The Minerals, Metals & Materials Series, Springer, Cham, 2019) https://doi.org/10.1007/978-3-030-05864-7_190.
34) C. Rochet, M. Veron, E.F. Rauch, T.C. Lowe, B. Arfaei, A. Laurino, J.P. Harouard and C. Blanc: Corros. Sci. **166** (2020) 108453.
35) IEC 62004:2007 *Thermal-resistant aluminum alloy wire for overhead line conductor*.
36) T.A. Latynina, A.M. Mavlyutov, M.Yu. Murashkin, R.Z. Valiev and T.S. Orlova: Philos. Mag. **99** (2019) 2424–2443.
37) T.S. Orlova, T. Latynina, M.Yu. Murashkin and V.U. Kazykhanov: Phys Solid State **61** (2019) 2509–2519.
38) T.S. Orlova, T.A. Latynina, A.M. Mavlyutov, M.Y. Murashkin and R.Z. Valiev: J. Alloy. Compd. **784** (2019) 41–48.
39) N. Belov, M. Murashkin, N. Korotkova, T. Akopyan and V. Timofeev: Metals **10** (2020) 769.
40) T.S. Orlova, T.A. Latynina, M.Y. Murashkin, F. Chabanais, L. Rigutti and W. Lefebvre: J. Alloy. Compd. **859** (2021) 157775.
41) M.Yu. Murashkin, A.E. Medvedev, V.U. Kazykhanov, G.I. Raab, I.A. Ovid'ko and R.Z. Valiev: Rev. Adv. Mater. Sci. **47** (2016) 16–25.
42) X. Sauvage, N. Enikeev, R. Valiev, Y. Nasedkina and M. Murashkin: Acta Mater. **72** (2014) 125–136.
43) I. Matveeva, N. Dovzhenko, S. Sidelnikov, L. Trifonenkov, V. Baranov and E. Lopatina: Development and research of new aluminium alloys with transition and rate-earth metals and equipment for production of wire for electrotechnical applications by methods of combined processing. Light metals 2012, (TMS 2013 Annual Meeting and Exhibition, March 3–7, 2013, Minerals, Metals and Materials Society, San Antonio) pp. 443–447. https://doi.org/10.1002/9781118663189.ch76.
44) L. Liu, J.T. Jiang, B. Zhang, W.Z. Shao and L. Zhen: J. Mater. Sci. Technol. **35** (2019) 962–971.
45) Q. Shao, E. Elgallad, A. Maltais and X.-G. Chen: Developing Al–Zr–Sc Alloys as High-Temperature-Resistant Conductors for Electric Overhead Line Applications. *Light Metals 2023*, ed. by S. Broek, TMS 2023, The Minerals, Metals & Materials Series, (Springer, Cham, 2023) pp. 1266–1272. https://doi.org/10.1007/978-3-031-22532-1_170.
46) M.Yu. Murashkin, D.I. Sadykov, A.M. Mavlyutov, D.K. Magomedova and V.U. Kazykhanov: J. Phys. Conf. Ser. **2231** (2022) 012005.
47) A.V. Nokhrin, G.S. Nagicheva, V.N. Chuvil'deev, V.I. Kopylov, A.A. Bobrov and N.Y. Tabachkova: Materials **16** (2023) 2114.
48) V.I. Dobatkin, V.I. Elagin and V.M. Fedorov: *Rapidly Crystallized Aluminum Alloys*, (VILS, Moscow, 1995) [in Russian].
49) N.O. Korotkova, N.A. Belov, V.N. Timofeev, M.M. Motkov and S.O. Cherkasov: Phys. Met. Metallography **121** (2020) 173–179.
50) M.Yu. Murashkin, I. Sabirov, A.E. Medvedev, N.A. Enikeev, W. Lefebvre, R.Z. Valiev and X. Sauvage: Mater. Des. **90** (2016) 433–442.
51) A.E. Medvedev, M.Y. Murashkin, N.A. Enikeev, R.Z. Valiev, P.D. Hodgson and R. Lapovok: J. Alloy. Compd. **745** (2018) 696–704.
52) A.E. Medvedev, M.Y. Murashkin, N.A. Enikeev, I. Bikmukhametov, R.Z. Valiev, P.D. Hodgson and R. Lapovok: J. Alloy. Compd. **796** (2019) 321–330.
53) A. Mohammadi, N.A. Enikeev, M.Y. Murashkin, M. Arita and K. Edalati: J. Mater. Sci. Technol. **91** (2021) 78–89.
54) N.A. Belov, A.N. Alabin, D.G. Eskin and V.V. Istomin-Kastrovskii: J. Mater. Sci. **41** (2006) 5890–5899.
55) W.W. Zhou, B. Cai, W.J. Li, Z.X. Liu and S. Yang: Mater. Sci. Eng. A **552** (2012) 353–358.
56) R. Guan, Y. Shen, Z. Zhao and X. Wang: J. Mater. Sci. Technol. **33** (2017) 215–223.
57) K.E. Knipling, R.A. Karnesky, C.P. Lee, D.C. Dunand and D.N. Seidman: Acta Mater. **58** (2010) 5184–5195.
58) V.N. Chuvil'deev, I.S. Shadrina, A.V. Nokhrin, V.I. Kopylov, A.A. Bobrov, M. Yu Gryaznov, S.V. Shotin, N. Yu Tabachkova, M.K. Chegurov and N.V. Melekhin: J. Alloy. Compd. **831** (2020) 154805.
59) N.A. Belov, A.A. Aksenov and D.G. Eskin: *Iron in Aluminium Alloys: Impurity and Alloying Element*, (CRC Press, London, 2002) p. 360.
60) K. Liu, X. Cao and X.-G. Chen: Metall. Mater. Trans. **43** (2012) 1097–1101.
61) A. Medvedev, M. Murashkin, N. Enikeev, E. Medvedev and X. Sauvage: Metals **11** (2021) 815.
62) V.A. Shabashov, I.G. Brodova, A.G. Mukoseev, V.V. Sagaradze and A.V. Litvinov: Phys. Met. Metallography **4** (2005) 66–67.
63) V.V. Stolyarov, I.G. Brodova, T.I. Yablonskikh and R. Lapovok: Phys. Met. Metall. **100** (2005) 182–191.
64) V.V. Stolyarov, R. Lapovok, I.G. Brodova and P.F. Thomson: Mater. Sci. Eng. A **357** (2003) 159–167.
65) J.M. Cubero-Sesin and Z. Horita: J. Mater. Sci. **48** (2013) 4713–4722.
66) J.M. Cubero-Sesin and Z. Horita: Metall. Mater. Trans. A **46** (2015) 2614–2624.
67) O.N. Senkov, F.H. Froes, V.V. Stolyarov, R.Z. Valiev and J. Liu: Scr. Mater. **38** (1998) 1511–1516.

68) A. Duchaussoy, X. Sauvage, K. Edalati, Z. Horita, G. Renou, A. Deschamps and F. De Geuser: Acta Mater. **167** (2019) 89–102.
69) A.E. Medvedev, M.Yu. Murashkin, N.A. Enikeev, R.Z. Valiev, P.D. Hodgson and R. Lapovok: Adv. Eng. Mater. **20** (2018) 1700867.
70) N. Belov, T. Akopyan, N. Korotkova, M. Murashkin, V. Timofeev and A. Fortuna: Metals **11** (2021) 236.
71) ASTM B800-05(2021) *Standard Specification for 8000 Series Aluminum Alloy Wire for Electrical Purposes—Annealed and Intermediate Tempers*.
72) G.L. Shuai, Z. Li, D.T. Zhang, Y.X. Tong and L. Li: Vacuum **183** (2021) 109813.
73) A.E. Medvedev, O.O. Zhukova, V.U. Kazykhanov, A.F. Shaikhulova, N.A. Enikeev, V.N. Timofeev and M.Yu. Murashkin: Int. J. Lightweight Mater. Manuf. **5** (2022) 484–495.
74) S.O. Rogachev, E.A. Naumova, E.S. Vasileva, M. Yu Magurina, R.V. Sundeev and A.A. Veligzhanin: Mater. Sci. Eng. A **767** (2019) 138410.
75) X. Sauvage, F. Cuvilly, A. Russell and K. Edalati: Mater. Sci. Eng. A **798** (2020) 140108.
76) L. Tian, A. Russell, T. Riedemann, S. Mueller and I. Anderson: Mater. Sci. Eng. A **690** (2017) 348–354.
77) I.A. Zhukov, A.A. Kozulin, A.P. Khrustalyov, A.E. Matveev, V.V. Platov, A.B. Vorozhtsov, T.V. Zhukova and V.V. Promakhov: Metals **9** (2019) 65.
78) Y. Qi, R. Lapovok and Y. Estrin: J. Mater. Sci. **51** (2016) 6860–6875.
79) Y. Koiwa, M. Sugawara and M. Fukuhara: SEI Tech. Rev. **90** (2020) 27–30.
80) R. Lapovok, M. Dubrovsky, A. Kosinova and G. Raab: Metals **9** (2019) 960.
81) R. Lapovok, V.V. Popov, Y. Qi, A. Kosinova, A. Berner, C. Xu, E. Rabkin, R. Kulagin, J. Ivanisenko, B. Baretzky, O.V. Prokof'eva, A.N. Sapronov, D.V. Prilepo and Y. Beygelzimer: Mater. Des. **187** (2020) 108398.
82) F. Moisy, A. Gueydan, X. Sauvage, A. Guillet, C. Keller, E. Guilmeau and E. Hug: Mater. Des. **155** (2018) 366–374.
83) C. Yang, N. Masquellier, C. Gandiolle and X. Sauvage: Scr. Mater. **189** (2020) 21–24.
84) M.Yu. Murashin and I.V. Smirnov: *High-strength aluminum-based composite heat-resistant wire*, Patent RU 2772800 C1 (2021).
85) E.A. Klimov and M.Yu. Murashkin: Nano Industry **14** (2021) 150–158.
86) E.I. Fakhretdinova, G.I. Raab and R.Z. Valiev: Adv. Eng. Mater. **17** (2015) 1723–1727.
87) E.I. Fakhretdinova, E.V. Bobruk, G.Yu. Sagitova and G.I. Raab: Lett. Mater. **5** (2015) 202–206.
88) Z. Horita, Y. Tang, T. Masuda and Y. Takizawa: Mater. Trans. **61** (2020) 1177–1190.
89) P. Kral, J. Dvorak, V. Sklenicka and T.G. Langdon: Mater. Trans. **60** (2019) 1506–1517.
90) P. Král, J. Dvořák, M. Kvapilová, M. Svoboda and V. Sklenička: Acta Metall. Slovaca Conf. **3** (2013) 136–144.
91) M. Kawasaki, V. Sklenička and T.G. Langdon: J. Mater. Sci. **45** (2010) 271–274.
92) R.A. Michi, J.P. Toinin, A.R. Farkoosh, D.N. Seidman and D.C. Dunand: Acta Mater. **181** (2019) 249–261.